Physics-based Surrogate Modeling of Impact Damage in Multi-material Laminates for Ultrasonic Diagnostics and ML Damage Prediction

Stefan Bosse[1,2], Christoph Polle[3]
[1]University of Koblenz, Dept. of Computer Science, Koblenz, Germany
[2]University of Siegen, Dept. of Mechanical Engineering, Siegen, Germany
[3]Faserinstitut Bremen, Bremen, Germany

Abstract. Non-destructive Testing and Structural Health Monitoring of damage require sufficient data and damage models on different scales. This work contributes to geometric physics-informed surrogate impact damage modeling of multi-material and multi-layer composites by introducing an alternative method to the intricate cohesive zone approach commonly employed in finite element analysis. The outlined approach and rigorous workflow establish a repeatable and clearly documented pipeline from CT scan analysis to validated synthetic damage models, which can be used for 1. enhancing the accuracy and calibrating of supervised machine learning algorithms for automated damage characterization, and 2. to create geometric damage models for (guided) Ultrasonic wave simulation used in Structural Health Monitoring applications, here specifically considering immersion measuring techniques to investigate impact damage. The data output of the Ultrasonic simulation is used to train a simple ML regression model predicting the original impact energy, demonstrating the requirement for data with dense and broad parameter spaces and a high degree of data variance.
Keywords: Structural Health Monitoring; Ultrasonic Monitoring; Impact Damage; Machine Learning; Surrogate Modeling; Physics-informed Modeling; Fiber-Metal Laminate; Simulation

1. Introduction

Modeling of impact damage in composite structure typically involves computation intensive Finite-Element Methods (FEM) analysis, as shown by Davies [1]. In damage diagnostics different phenomena are of interest to assess such a composite (multi-layered) structure (as described by Shah et al. [2]):

1. Inner layer effect: Cracks inside a layer (e.g., commonly in brittle materials like glass);
2. Inner layer effect: Deformation of (plastic) materials, e.g., like in metals;
3. Intra-layer effect: Full delamination (with void volume between layers);
4. Intra-layer effect: Partial delamination (without void between layers, but without contact/adhesion, i.e., so called kissing-bond defects).

Two prominent measuring methods can bes considered for the diagnostics of hidden defects: 1. X-ray Computed Tomography (CT), 2. Guided, transmission, or pulse-echo Ultrasonic wave (UW) monitoring. CT can be used to detect phenomena 1, 2, and 3, whereas US can be used to detect phenomena 4, too. These methods can be used in disjunction or in conjunction (fusion), as Katunin et al. [3] demonstrated.

Leonard et al. [4] investigated damage caused by impact events using X-ray CT in composite materials (carbon fiber reinforced polymer, CFRP) and found significant breakage and cracks in the the fiber layers. A synthetic damage model for such fine-grained and random damage can be created by using stochastic models and Monte Carlo simulation assisted by a physical model, but showing high computational complexity and a large reality gap can be expected. We consider metal-fiber laminates, where we consider and investigate the deformation and delamination. In this work we address the modeling of the deformation of individual layers of a multi-layer and multi-material laminate structure with a physics-informed surrogate or helper model, specifically for Fiber Metal Laminates (FML). This model bases on a simple mass-spring multi-body model that is responsible to model the deformation of one layer by using a shape generator function. This model approach is superior compared to FEM methods with much lower computation complexity. The entire approach in this work consists of analytical investigations of real damages for the parameterization and calibration of the synthetic damage model. This deformation model is capable to create different geometric output models that can be processed by X-ray simulation or Ultrasonic simulation. One advantage of our approach compared with FE analysis is the low computational complexity and computational time.

Deformation of non-compressible materials underly the constant mass-volume constraint, which must be satisfied by the deformation model, too. Deformation of multi-layer structures, e.g., FML, must additionally satisfy collision-free deformation of individual layers, i.e., without intersection of layers. It can be shown that the simple physical surrogate damage model introduced in this work satisfies these constraint. The damage model bases on a simple coupled mass-spring model (multi-body physics). It can be used to calculate deformation of multi-layer structures caused by impact events without violating geometric constraints. The model is parameterizable by fixed (static) material and structure parameters, e.g., calibrated by CT analysis, and dynamically by control parameters like the impact energy, deformation size, and deformation skewness.

In previous work (Kumar et al. [5]) a predecessor damage model was used to carry out X-ray simulation to generate synthetic data for the training and calibration of Deep ML-based feature marking models applied to X-ray CT scan data. In this work, an extended and improved damage model is introduced and used to carry out Ultrasonic wave simulation to generate synthetic data for the training of a simple ML-based regression model. The output of the regression model is the energy of the impact event. To demonstrate the benefit of the damage simulation model, we apply the output of the damage simulator to Ultrasonic wave simulation of a common immersion measuring experiment, computing the wave propagation through the cross section of the multi-layer material. The novelty of the damage model introduced in this work compared to the previous model in [5] is the extension to enable model calibration directly from X-ray CT analysis of real impacted specimens, the control of the model by the impact energy and the initial impact radius, the support of multi-material layer compositions with different deformation behavior, and geometric damage skewness controlled by only one model parameter.

Immersion ultrasonic measurement techniques are used for impact detection and qualification in FML. In these methods, the specimen is immersed in water, which serves as a coupling medium for efficient transmission of ultrasonic waves. Different measurement and data processing methods can be used for damage detection. The most known are the A-, B- and C-scans, which are described in Tab. 1. High excitation frequencies in the range of 2–10 MHz are typically used for plate-like structures, as they provide sufficient spatial resolution to detect small-scale defects such as delamination. However, higher frequencies also lead to increased attenuation, particularly in anisotropic materials such as FML, which limits penetration depth.

Method	**Description**	**Advantage**	**Disadvantage**
A-Scan	One dimensional representation of echo pulse amplitudes as a function of time (depth scan).	Fast and easy measurement with a high depth resolution and small amount of data.	Delivers no area information; data interpretation is difficult and needs experience.
B-Scan	Two-dimensional cross-sectional view (depth vs. scan position).	Visualization of defects and discontinuities in over the depth; more intuitive as a-scans.	Limited area information; less overall view than C-scan
C-Scan	Two-dimensional area representation in which reflected ultrasonic signals are mapped over the scanned surface.	Provides a clear overview of defect size and distribution; ideal for delamination.	Normal no direct depth information, unless time-of-flight gating (D-scan) is applied; often time-consuming

Tab. 1. Comparison of different immersion ultrasound scan techniques [6]

Among these techniques, the C-scan is one of the most widely used methods for damage detection in composite materials such as FML. Gyekanyesi et al. [7] used C-scans to quantify impact damage in GLARE and ARALL specimens. The study performed different experiments with several variable parameters, like impact velocity, mass (of impactor), temperature, laminate configuration and sandwich construction. With the C-scans, a variety of different damage patterns, like plastic deformation, cracks, partial and full delamination, could be identified in the impact area. The correlation between impact energy and delamination area in GFRP specimens was investigated by Naik et al. [8]. The delaminations were clearly visible in the C-scans, and it was found that the delamination area increases with the impact energy. However, the study of Blackman et al. [9] showed that C-scans seem to underestimate the size of foreign object defects in CFRP specimens. The results could be optimized after using the developed maximum gradient transition (MGT) method.

Another widely used method is the B-scan. Ni et al. [10] used simulation and experimental data to optimize b-scans for CFRP specimens since classical b-scans produce errors in anisotropic laminates. Since b-scans show cross sections of the specimen, they are particularly useful for analyzing the depth distribution of defects. But in anisotropic materials such as FML, b-scans can lead to distortions. In order to address this problem, advanced reconstruction techniques such as the Total Focusing Method (TFM) were developed, which improve image quality by considering directional wave propagation. TFM was further optimized in [10] by taking the fiber angle and the directional wave velocity into account. In [3] a method was introduced where B- and C-scans have been merged to detect barely visible damage in CFRP specimens. As reference, CT scans were used. Due to the fusion of the two ultrasonic scan methods, a 3D representation of the damage was possible.

In summary, it can be noted that in structures with altering material layers like in FML the analysis of immersion ultrasonic measurements can be challenging. This is due to complex wave interactions with the different material layers, as well as the influence of anisotropy introduced by fiber orientations. In order to deal with this problem different advanced signal processing and imaging techniques, like data fusion and TFM have to be developed. To achieve this, and given the growing use of machine learning in this field, enormous amounts of data are required. Increasingly, this data will need to be obtained through simulation and data augmentation, as the sheer volume of data required cannot be provided by experiments alone.

2. Methods and Models

2.1 Damage Model

We consider impact damages applied to one side of a plate. The impact event, e.g., caused by a steel ball with a specific kinetic energy E, will cause deformation of the plate. If the plate consists of different layers and different materials, the deformation can cause delamination. The modeling and calculation of the deformation is a challenge. The calculation of the deformation must satisfy different constraints (assuming non-compressible materials like metals or glasses):

1. The mass-volume must be constant, i.e., the deformation will not change the mass and the enclosing volume of a layer;
2. The deformation can be partially temporary (elastic deformation), e.g., in the case of glasses, or permanent, e.g., in the case of metal (inelastic deformation). Therefore, different deformation models are required for different materials.
3. The thickness of a deformed layer will not be constant along the horizontal and vertical axis of the plate, i.e., deformation thins the layer (about 1-10%) because the layer surface area increased, but still preserving constraint 1!
4. Layers may not intersect after the impact event and the individual deformation.

The layer profile with an impact damage can be modeled by a parameterized bell (Gaussian) curve with sufficient accuracy, as found by µCT analysis from damaged FML specimens, and discussed in Sec. 3. The deformation can be symmetric to the orthogonal axis of the plate or asymmetric. Asymmetry can be covered by a skewed Gaussian function. The mathematical generator function *G* for the deformation of each layer is given by:

$$
\begin{gathered}
G(x, x_0, \sigma, \alpha) = k e^{-\frac{(x-x_0)^2}{2(\sigma+\alpha(x-x_0))^2}} \\
L_i(y_0, D_i, S_i) : \mathbb{R}^3 \to \mathbb{R}^{W \cdot H} \\
L_i(y_0, D_i, S_i) = \left\{ S_i G\left(x, \frac{W}{2}, D_i, \alpha\right), x \in \{0, 1, .., W-1\} \right\} \\
i \in \{1, 2, ..\}, D_i = D \cdot T_x^i, S_i = S \cdot T_y^i
\end{gathered} \tag{1}
$$

with σ as the normalized width of the bell curve and α as the skewness parameter in the range [0,1]. The generator function *G* is applied to each layer, discretized by *W* points, and commonly increasing the width and slightly the height of the deformation, given by the variable *D* and *S*, increases by each layer by factors T_x and T_y, respectively.

The naive approach is the application of the same bell curve to the lower and upper side of a plate layer, which is not physically consistent. If the deforming forces are applied to the lower side of the plate with a specific bell curve of width σ_1 and height β_1, then the upper bell curve will have different parameters, typically $\sigma_2 > \sigma_1$ and height $\beta_2 < \beta_1$, i.e., a slight broadening and flattening of the upper side will result.

To satisfy the above constraints, we use a physical mass-spring model to simulate the deformation of single layers of a single- or multi-layer plate, as shown in Fig. 1, composing a multi-layer mass-spring model. Each layer consists of mass nodes connected by springs with a specific spring constant. The generator function is only applied to the lower side nodes, the other nodes are moved according to Hookes law. Instead positioning the lower side nodes directly, they are coupled to a hidden set of fixed nodes, those positions are determined by the generator function. The fixed nodes are coupled via springs to the layer nodes, too. The unified mass of each node was set to 0.001 (arbitrary units), which is not relevant for the stationary state (gravity is not considered). The fixed nodes are assigned to infinity mass.

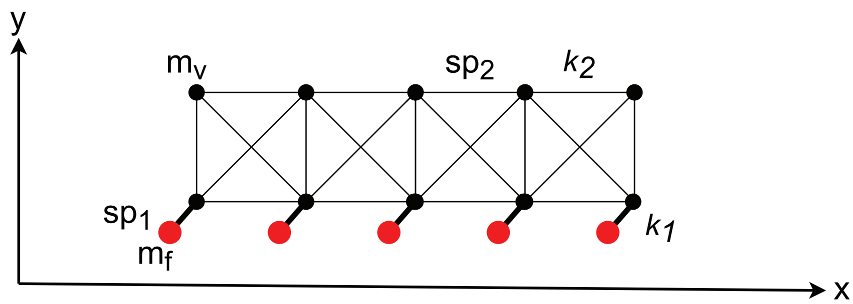

Fig. 1. Basic two-dimensional mass-spring mesh-grid model of one layer. There are elastic nodes (m_v) and fixed nodes (m_f), each class connected by springs sp_1 and sp_2 with spring

constants k_1 and k_2, respectively. The fixed nodes drive the bottom node row, finally moving the upper node row.

This model is still oversimplified as it can be seen form the µCT results of real samples presented in this work. But this simplified model can be used to evaluate and calibrate the feature marking models (considered as a gold standard) because the geometric damage characteristics can be calculated from the numerical material model. A layer must consists at least of two rows of mass nodes. More rows increase the elastic deformation capability.

At least two vertical nodes are required, but a larger number of vertical nodes per layer group can be modeled, too. A higher number of vertical (and horizontal) nodes results in a more realistic and accurate deformation shape.

Note that solving the multi-body physics problem is an iterative (time-dependent) process. The computation is fast (commonly requires less than 1 ms), but requires the (algorithmic) observation of a sufficient stop condition of the iterative physics simulation, which is performed via a time- and spatially averaged mass movement of the model.

2.2 Area of Polygons and Volume of Revolved Polygons

The layer area and revolved volume computation is used for the evaluation of the accuracy of the damage model and the fulfillment of constraints. The area (or volume) of a deformed layer must be equal to the area (or volume) of an undeformed layer to satisfy the constant mass-volume constraint.

For each layer we have a point list P forming the outside polygon of the layer. Each point has a x- and y-coordinate. The area of a hull polygon is calculated by:

$$
\begin{gathered}
P = \{\vec{p}_i, i = 1..n\} \\
A(P) = \left| \sum_{i=1}^{n} \frac{x(\vec{p}_i)y(\vec{p}_{i+1})}{2} - \frac{x(\vec{p}_{i+1})y(\vec{p}_i)}{2} \right|, p_0 = p_n, p_{n+1} = p_1
\end{gathered} \tag{2}
$$

To get measure in the third dimension, this layer polygon can be rotated around the y-axis (solid revolution).

The volume of such a rotated solid can be calculated by Passu's theorem by:

$$
\begin{gathered}
V_y = \pi A(P_h) c_x \\
P = \{\vec{p}_i, i = 1..2n\} \\
P_h = \{\vec{p}_i \in P, x(\vec{p}_i) \geq 0\} \\
y_0 = \min\left(y(P_h)\right) \\
d_x = \frac{1}{n}\sum_{i=1}^{n} x(\vec{p}_i), p_i \in P_h \\
d_y = \frac{1}{n}\sum_{i=1}^{n} y(\vec{p}_i) - y_0, p_i \in P_h \\
c_x = \sqrt{d_x^2 + d_y^2}
\end{gathered} \tag{3}
$$

with c_x as the distance of the y-axis to the centroid point of the layer shape (right half side, $p(x) \geq 0$, assuming rotation in the center of the layer shape), $p(x)$ the x-position of polygon point p, and A as the area of the layer.

2.3 Damage Modeling

From X-ray CT-analysis the following formulas were derived describing the change of the deformation parameters width and height through the layers:

$$
\begin{gathered}
dx_i = D \cdot T_x^i \\
dy_i = S \cdot T_y^{(i\%2)g+(1-(i\%2))}, g < 1 \\
D = R\frac{W}{sc} \\
S = c_0\sqrt{\frac{E}{k_3}} \\
T_X = c_1 + k_1\sqrt{\frac{E}{k_3}} \\
T_y = c_2 + k_2\sqrt{\frac{E}{k_3}} \\
c_0 = 1.5, c_1 = 1.1, c_2 = 1, k_1 = 0.1, k_2 = 0.2, k_3 = 10
\end{gathered}
\tag{4}
$$

The coefficients are only examples and specimen specific (layer composition, geometric parameter).

The input parameters of the damage model are the impact energy *E* (J) and the initial geometric impact radius *R* (mm), in an impact experiment typically the radius of the impacting ball. The coefficients *c*, *g*, and weights *k* must be calculated from X-ray CT analysis of specific specimens. It is assumed that there is an alternating layer material composition metal/glass, i.e., layer with index 0 is metal, layer with index 1 is glass, and so forth. The different material behavior is reflected by the modulo operation `%`. Metal shows stronger plastic deformation than glass. The width *W* is the number of nodes in x-direction of the surrogate model, and *sc* the scale (mm) with respect to *W*, i.e., a scale 1 means a physical width of 50 mm with *W*=50.

2.4 Examples

Fig. 2. shows two example computation for a 5-layer laminate with alternating metal-glass materials using the damage model for an impact energy *E*=20J and without and with skewness. The model parameters were calibrated by CT analysis of real specimens. Every second layer is glass material with reduced deformation compared with the metal layer, i.e., during the impact the glass layers are deformed the metal layers, but afterwards they partially relaxed back. For higher impact energies cracks are created, which are not modeled in this work.

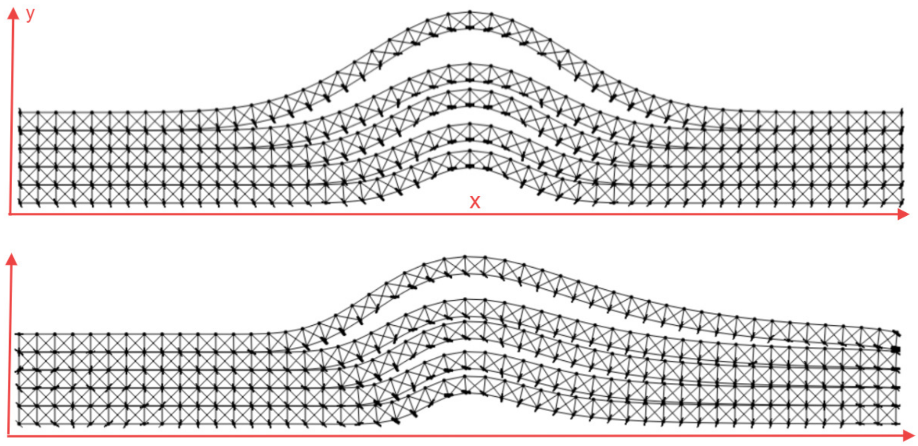

Fig. 2. Example damage generation with five layers (alternating metal/glass material), E=20 J, R=5 mm, sc=50/mm. (Top) Skewness A=0 (Bottom) Skewness A=0.2

2.5 Simulation

The output of the geometric damage model is a two-dimensional layer cross section of the composite material, describing layers by hull polygons (position of outer nodes of the mass-spring model). This two-dimensional polygon-point map can be used directly for physical simulation, two-dimensional, e.g., cross-sectional Ultrasonic wave propagation simulation by creating a material matrix, or for a three-dimensional physical simulation, e.g., X-ray projection image simulation (radiography as well as CT) by using three-dimensional modeling methods like revolving of the polygon shapes:

1. Ultrasonic wave simulation with the SimNdt2b simulation toolkit uses a regular two-dimensional material matrix as input, directly derived from the layer shapes. The material properties are taken from material parameter tables (i.e., density, wave velocities, damping factors and so on). The SimNdt simulator [11], originally created by Molero [12], uses a parallel implementation of Viscoelastic EFIT (Elastodynamic Finite Integration Technique), applied to a discrete two-dimensional grid, created from material matrix. Our SimNdt2b successor is fully batch script driven and provides extended input and output interfaces optimized for large data set generation.
2. X-ray simulation (transmission projection images) with the gVirtualXray simulation toolkit [13] uses a three-dimensional mass density tensor volume, computed by Constructive Solid Geometry operations (translation, rotation/revolving). The CSG model can be directly derived from the computed layers polygons. The gVirtualXray simulator bases on ray tracing, as introduced by Vidal et al. [14].

Fig. 3 shows the four parts of our work, starting from X-ray CT analysis for the model calibration, the damage model simulator with model validation (physical constraint checks) and the mapper functions generating models that can be used by the target simulation.

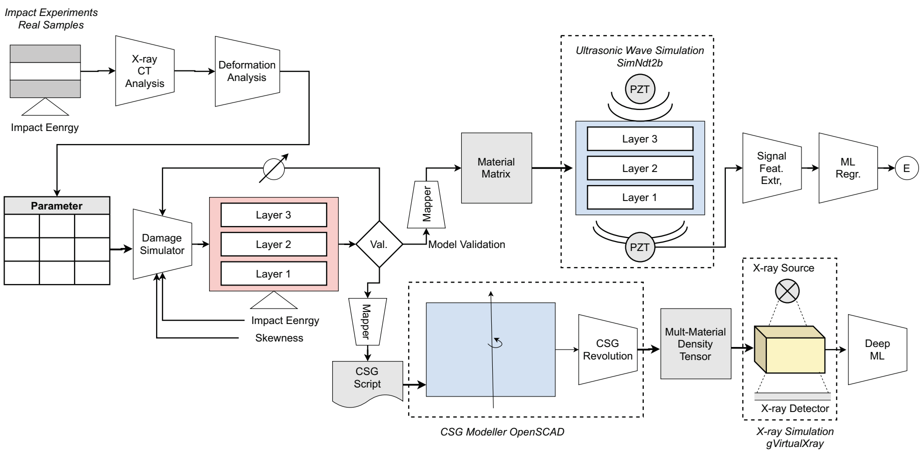

Fig. 3. Overview of the full workflow incorporating the damage model. Results of the geometric damage simulation is used for physical simulations (Top, right) 2-dim Ultrasonic wave simulation with SimNdt2b (Bottom, right) 3-dim X-ray simulation with gVirtualXray. Damage model parameters are derived from X-ray CT analysis and image processing (demonstrated in [5]).

For the sake of simplicity we will test our model for immersion Ultrasonic wave simulation, finally using the signal output from the US simulation to train a simple data-driven ML model that should be capable to predict the original impact energy from only three transducer signals. The experimental set-up is explained in Sec. 3,

2.6 Data-driven Damage Predictor Model

To demonstrate the usefulness of the proposed physically-informed damage simulator for the generation of large synthetic data sets with high parameter variance we will derive relevant features from Ultrasonic signals in an immersion measuring set-up. The output of the predictor model is the impact energy *E*, the input are relevant features of three time-resolved Ultrasonic signals.

Investigation of the dependency of the damage area from the impact energy performed by Sultan et. al [15] showed that the area is nearly proportional to the impact energy. We assume that an increasing delamination area and a corresponding delamination volume between layers have an increasing impact on the wave propagation and being the relevant physical part of the damage-wave interaction, here assumed as air (although, commonly vacuum, but this cannot be simulated due to discontinuity)). We identified the time delay of the first wave at 10% amplitude normalized to the maximum of the hull of the wave group as the relevant signal feature, assuming a discrete signal s.

$$
\begin{aligned}
s &= \{s_i, 1 \leq i \leq m\}, s(n) \approx s(t) \\
s_{\max} &= \max\left(|z(s)|\right) \\
z(s) &= s + ih \\
h(k) &= \begin{pmatrix} \frac{2}{\pi}\sum_{n=1,3,..}\frac{s(n)}{k-n} & k\%2=0 \\ \frac{2}{\pi}\sum_{n=2,4,..}\frac{s(n)}{k-n} & k\%2=1 \end{pmatrix}
\end{aligned}
\tag{5}
$$

with h as the discrete Hilbert transform and z the discrete analytical signal.

Fig. 4 shows the relation of the wave time delay t_d with the impact energy for the three receiver signals (left, center, right), calculated from signals from the US simulation. The center signal has nearly a linear relation of the delay in the range [2J,8J] impact energy, the left and right signal delays have a nearly linear relation above 7J, covering together a high correlation between the impact energy and the signal delay.

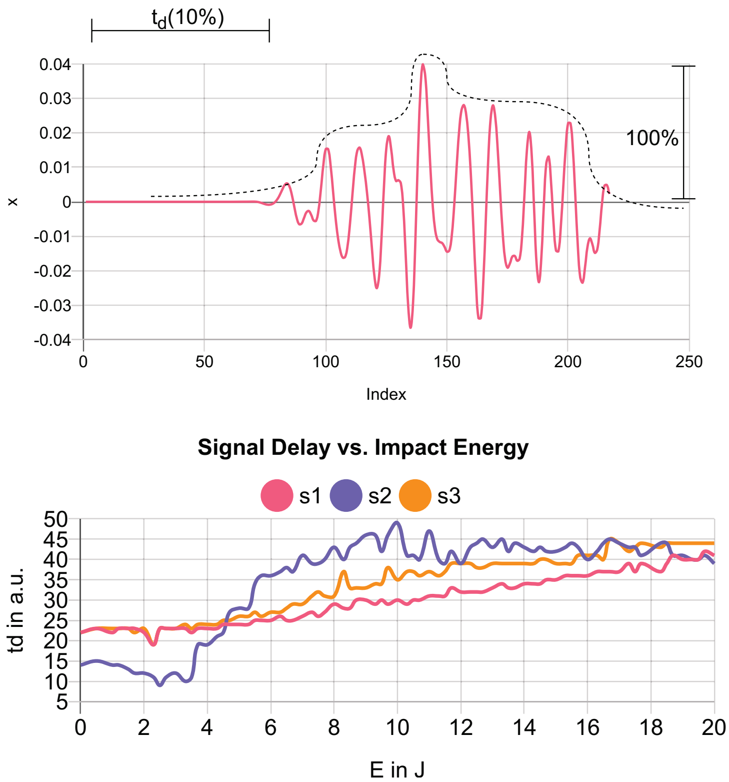

Fig. 4. (Top) Example signal and definition of delay time t_d. by using the hull computation via the analytical signal. (Bottom) Relation of the wave time delay t with the impact energy for the three receiver signals (left, center, right) for different impact energies (symmetric damages, i.e., A=0).

There is still a non-linear relationship between the three feature variables t_1, t_2, and t_3, but a small non-linear function approximation model like a FCANN with two or three layers and less than 10 neurons per layer is sufficient, as shown in Sec. 3.

3. Experiments and Results

3.1 μCT Investigation

The X-ray μCT investigation is used in this work to extract the relevant damage model parameter:

1. The change of hight and width of the damage deformation for each layer;
2. Capturing different material behavior, i.e., different relative deformation with respect to the material classes metal and glass with and without plastic behavior;
3. Geometric calibration of the synthetic damage model (layer shape).

Fig. 5 shows examples of material slices of baseline and damaged specimens with different impact energies. For each layer a hull polygon was computed semi-automatically by using edge detection algorithms (Canny-based) and visual inspection to avoid false marking of cracks and CT artifacts. The contour of each layer was reconstructed and geometric measures calculated, i.e., deformation height and width, skewness, and the fitting of parameters of the generator function were optimized. The results of the CT analysis are used for the damage simulation, discussed in the next section. The CT scans were computed from (1000) projection X-ray images captured with an Zeiss Xradia μCT device at the University of Siegen, delivering a theoretical voxel resolution of about 30 μm. The plate had a total thickness of about 5 mm.

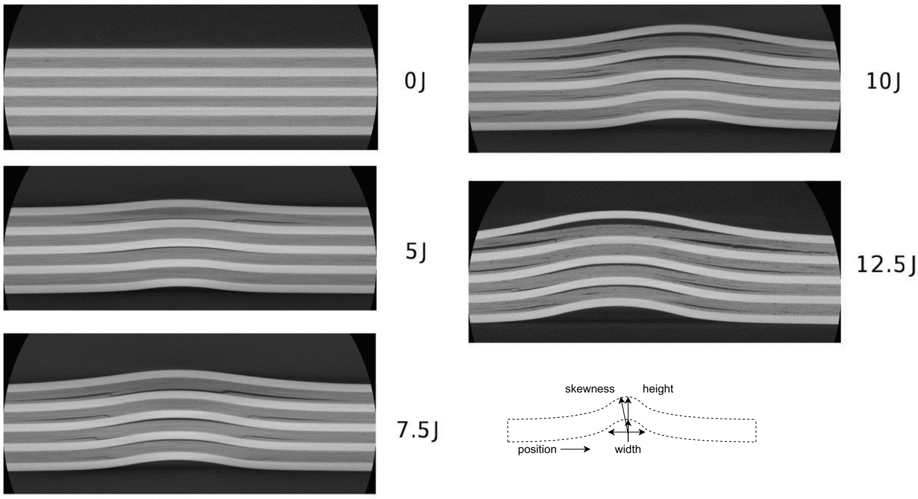

Fig. 5. Different μCT slices from a FML plate with impact damages caused by different impact energies (sphere hammer). At higher energies an asymmetric deformation is created. The FML consists of Aluminum and glass fiber resin layers. The CT slices were used to calculate the damage model parameters.

3.2 Damage Simulation

For the sake of simplicity we reduced the number of layers to 5 with the material configuration [Al,Gl,Al,Gl,Al], where solid glass material replaced the original complex glass fiber-matrix structure. A large set of 200 different plates with one impact damage per plate were simulated. The impact energy range was chosen with E=[0 J,20 J] for three skewness parameters A={0,0.1,0.2}, based on CT specimens with discrete energies 0, 5, 7.5, 10, and 12.5 J. used for model calibration. The test specimen consists of five layers with material configuration [A,G,A,G,A] (A: Aluminum, g: glass). The output of the damage simulator is a material index matrix (cross section of the deformed plate) that can be directly used by the Ultrasonic simulator introduced next. The thickness of the plate was scaled to 10 mm. Each layer was modeled with 50 horizontal and 2 vertical nodes. The physical scale was 2 mm / grid point. The normalized spring constants were k_1=50 and k_2=70 for fixed and free node connections, respectively. Additionally, the damage simulator outputs the material matrix as an image.

3.3 Ultrasonic Wave Simulation

We will use a simple Ultrasonic wave simulator, SimNdt2b [11], to demonstrate the usage of our impact damage simulator, which is limited to the simulation of wave propagation in a two-dimensional grid by solving non-linear wave propagation equations. The limitations of two dimensions forced us here to a simple immersion transmission experiment, embedding the FML plate in water. We have placed one sending transducer on the top side of the plate, and three receiving transducers on the bottom side of the plate, all separated from the plate by water.

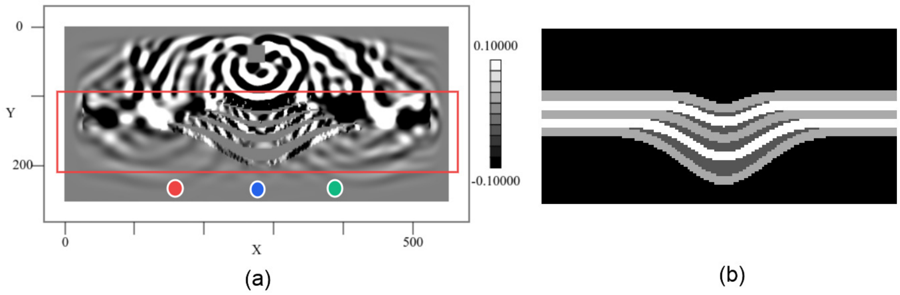

Fig. 6. (a) Snapshot of the two-dimensional wave field computed by SimNdt2b [11] for a plate with an impact damage caused by E=20 J. The position of the three receiving transducers are show on the bottom, too. The red rectangle encloses the plate. The width pf the plate is 100 mm and the height (without damage) is 10 mm. (b) The material grid used for the simulation computed by the damage simulator (black: water, light grey: Aluminum, white: glass, dark grey: air)

3.4 Damage Prediction

The fully connected Artificial Neuronal Network (FCANN) ML model is a regression model with three FC layers with [10,5,5] neurons and sigmoid activation functions. The ML model was trained with samples without damage skewness and an impact energy range [0J,20J]. The model was tested with additional samples in the impact energy range [0J,20J] and a skewness of A=0.1 and A=0.2. Fig. 7 shows prediction results. Because this model is used only for a demonstration and the proof-of-concept no statistical analysis of the model was performed. Even with this simple experiment we can identify that skewness of the damage (which can be expected in any real-world impact event) creates a strong deviation of the energy prediction of the ML model for higher energies (> 7J). If the model is trained with samples having a skewness variance (A=0,0.1,0.2), as shown in Fig. 8, the prediction quality increases for skewed damages, but still with a deviation in the mid energy range. It can be concluded that the prediction model is still specialized and cannot capture the parameter variance entirely.

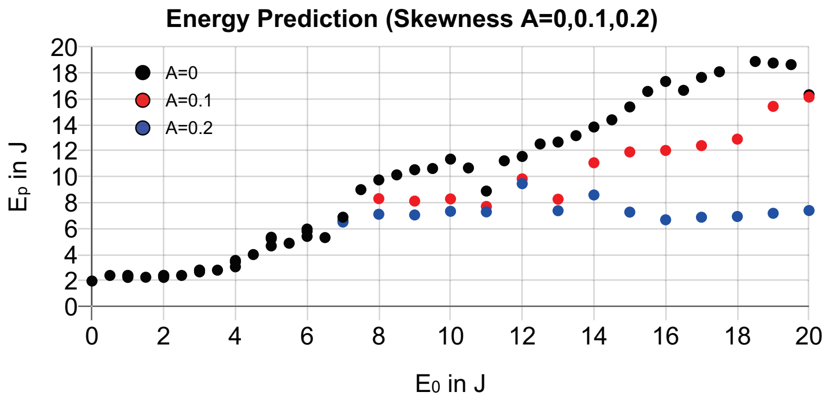

Fig. 7. Experiment 1: Results of the energy prediction from three transducer signals by using the signal delay as input variables. E_0 is the energy parameter of the damage simulation, and E_p the predicted value of the ML model from the signal delay features. The training was performed with A=0 samples only. The test was performed with additional samples having a skewness factor of A=0.1 and A=0.2, showing strong deviations in the prediction results for higher energies (> 7J).

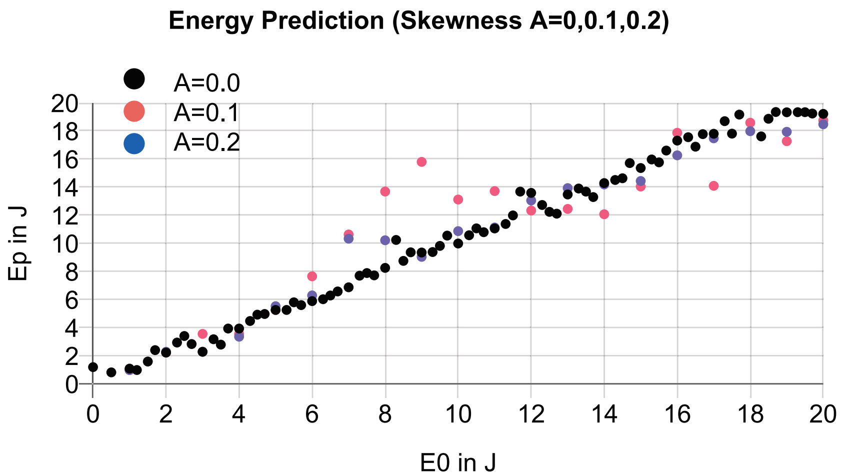

Fig. 8. Experiment 2: Results of the energy prediction from three transducer signals by using the signal delay as input variables. E_0 is the energy parameter of the damage simulation, and E_p the predicted value of the ML model from the signal delay features. The training as well as the test were performed´with all samples having a skewness factor of A=0, A=0.1, and A=0.2, showing better conformance in the prediction results, but still with deviation in the mid-range.

4. Evaluation and Conclusion

The physics-based geometric impact damage model can be parametrized and calibrated providing sufficient accuracy for the computation of the deformation of layers after an impact event within a wide energy E range. The static damage model parameters are derived from X-ray CT image analysis of real impacted specimens. A mass-spring (multi-body) model is used to simulate the deformation of a layer driven by a generator function. The aim of the simplified surrogate damage model is the generation of large data sets, used, e.g., for ML tasks, providing a broad and dense parameter space and a high sample variance.

The constant mass-volume (or here area) constraint is satisfied with a maximal increase of the area of about 1% and evolved volume of about 2.5% up to an impact energy of E=20 J (with two vertical and 50 horizontal model nodes per layer slice). The number of nodes in the surrogate model can be increased to improve the deformation simulation. The damage model shows low computational complexity and computation times (a few ms).

The damage simulator can be used to directly create discretized two-dimensional material distributions of the cross-section of a multi-layer material as well as indirectly three-dimensional material distributions by using CSG and revolving of layer cross section polygons. All relevant geometric quantities can be directly computed by the damage simulator, e.g., delamination volumes or distances between layers. The Area of Coverage (AoC) of the simulated damage patterns is about 70% compared with cross-sections of real specimens, providing sufficient accuracy for the generated synthetic data.

An Ultrasonic wave simulation was used to simulate simple immersion experiments of impacted plates (surrounded by water). We used one sending transducer and three receiving transducers to measure the signal response. The time delay of the signals were identified as major features derived from the normalized signal hull and computed by using the Hilbert transform. The time delays were used as the input to a simple ML regression model, which should predict the original impact energy. We created a large sample set (N=200) with energies in the range E=[0,20J] and different skewness parameters A=0,0.1, and 0.2.

We performed two ML-based data analysis experiments using the synthetic data generated by the damage simulator: 1. Training of a ML regression model with samples having only skewness A=0, and testing with all samples, and 2. Training of the ML model with all samples (and different skewness). It is important to clarify that this is just a proof-of-concept experiment, so we did no statistical analysis of the trained model. But first outcomes show a relevant insight in ML modeling and data variance. The first ML experiment created a model that was able to predict the energy with sufficient accuracy (error less than 20%). But the prediction results for the samples with geometric skewness degrades rapidly for higher energies (and increased deformation), making the model nearly unusable (low generalization degree). If the model is trained with the skewed samples, too, the overall prediction quality improves significantly, but still showing deviation in the mid range without physical explainability.

In summary, this work showed with a simple surrogate model and the use-case of Ultrasonic simulation for ML-driven damage diagnostics the requirement of a dense and broad parameter space not accessible in this extend by real experiments, especially considering impact damage. The proposed damage model can decrease the reality gap and can be used to investigate ML models used for damage prediction, finally creating more generalized data-driven prediction models used in SHM.

In contrast to earlier work [5] where the model output was used for training of Deep Learning feature marking models applied directly to CT image data, the pure symmetric damage model (A=0) was sufficient.

One major issue of the damage model is its limitation to two-dimensional shapes. Although, CSG revolution can be used to create three-dimensional bodies, the rotation is limited to symmetric deformations (i.e., skewness A=0). One outcome is the migration from a two-dimensional to a three-dimensional mass-spring model and a three-dimensional (skewed) Gaussian generator function, which will be implemented and evaluated in the future.

5. References

1. Davies, G. A., Zhang, X., Zhou, G., Watson, S. (1994). Numerical modelling of impact damage. Composites, 25(5), 342-350
2. Shah, C., Bosse, S., von Hehl, A., Taxonomy of Damage Patterns in Composite Materials, Measuring Signals, and Methods for Automated Damage Diagnostics, Materials 15 (MDPI), no. 13 (2022): 4645
3. Katunin, A., Wronkowicz-Katunin, A., Dragan, K. (2020). Impact damage evaluation in composite structures based on fusion of results of ultrasonic testing and X-ray computed tomography. Sensors, 20(7), 1867.
4. Léonard, F., Stein, J., Soutis, C., Withers, P. J. (2017). The quantification of impact damage distribution in composite laminates by analysis of X-ray computed tomograms. Composites Science and Technology, 152, 139-148.
5. Kumar, S., Bosse, S., Shah, C. (2025), Investigation of deep learning approaches for automated damage diagnostics in fiber metal laminates using Detectron2 and SAM, Front. Artif. Intell. 8:1599345. doi: 10.3389/frai.2025.1599345
6. Jodhani, J., Handa, A., Gautam, A., Rana, R, Ultrasonic non-destructive evaluation of composites: A review, Materials Today: Proceedings, Volume 78, Part 3, 2023, Pages 627-632, ISSN 2214-7853, https://doi.org/10.1016/j.matpr.2022.12.055.
7. Gyekanyesi, J., Liaw, B., Villars, E., Delmont, F. (2003). Ultrasonic assessment of impact-induced damage and microcracking in polymer matrix composites. NASA Technical Report (NASA/CR-2003-63103).
8. Naik, H. R. M., Jerald, J., Mathivanan, N. R. (2012). Impact damage detection in GFRP laminates through ultrasonic imaging. Advanced Materials Research, 585, 337–341.
9. Blackman, N. J., Jack, D. A., Blandford, B. M. (2021). Improvement in the quantification of foreign object defects in carbon fiber laminates using immersion pulse-echo ultrasound. Materials, 14(11), 2919. https://doi.org/10.3390/ma14112919
10. Ni, F., Cao, A., Xu, H., Zhang, Z., Li, W., Su, Z. (2026). Ultrasonic inspection of delaminations in thick composite structures with variable fiber angles using optimal total focusing method: Simulation and experiment. Engineering Structures. https://doi.org/10.1016/j.engstruct.2026.122252

11. SimNdt2b, Advanced Ultrasonic NDT Simulator software with engine core based on the Elastodynamic Finite Integration Technique (2026), http://git.edu-9.de/sbosse/simndt2b, accessed on-line at 1.3.2026

12. Molero-Armenta, M., Iturrarán-Viveros, U., Aparicio S., Hernández, M.G., Optimized OpenCL implementation of the Elastodynamic Finite Integration Technique for viscoelastic media, Comput Phys Comm 185 (2014) 2683-2696.

13. gVirtualXRay, Advanced X-ray simulator software (2026), http://git.edu-9.de/sbosse/XraySim, accessed on-line 1.3.2026,

14. Vidal, Franck P, et al. X-ray simulations with gVXR in education, digital twining, experiment planning, and data analysis, Nuclear Instruments and Methods in Physics Research Section B: Beam Interactions with Materials and Atoms 568 (2025): 165804. https://doi.org/10.1016/j.nimb.2025.165804

15. Sultan, M. T. H., Worden, K., Staszewski, W. J., Pierce, S. G., Dulieu-Barton, J. M., Hodzic, A., (2009). Impact damage detection and quantification in CFRP laminates; a precursor to machine learning.